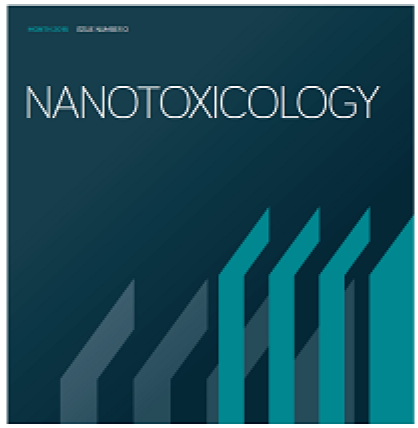

In vitro and in situ experiments to evaluate the biodistribution and cellular toxicity of ultrasmall iron oxide nanoparticles potentially used as oral iron supplements.

Journal:	*Nanotoxicology*
Manuscript ID	TNAN-2019-OR-0207.R1
Manuscript Type:	Original Article
Date Submitted by the Author:	n/a
Complete List of Authors:	Garcia Fernandez, Jenifer; Universidad de Oviedo, Department of Physical and Analytical Chemistry Turiel Fernandez, Daniel; Universidad de Oviedo, Physical and Analytical Chemistry Bettmer, Jorg; Universidad de Oviedo, Department of Physical and Analytical Chemistry Jakubowski, Norbert; Bundesanstalt für Materialforschung und -prüfung, Chemistry Panne, Ulrich; Bundesanstalt für Materialforschung und -prüfung, Chemistry Rivas Garcia, Lorenzo; Universidad de Granada, Department of Physiology Sanchez-Gonzalez, Cristina; University of Granada, Department of Physiology Llopis, Juan; Universidad de Granada, Department of Physiology Montes-Bayon, Maria; Universidad de Oviedo, Department of Physical and Analytical Chemistry
Keywords:	iron nanoparticles, intestinal perfusion, anaemia, mass spectrometry
Abstract:	Well-absorbed iron-based nanoparticulated materials are a promise for the oral management of iron deficient anaemia. In this work, a battery of in vitro and in situ experiments are combined for the evaluation of the

	uptake, distribution and toxicity of new synthesized ultrasmall (4 nm core) Fe2O3 nanoparticles coated with tartaric/adipic acid with potential to be used as oral Fe supplements. First, the in vitro simulated gastric acid solubility studies by TEM and HPLC-ICP-MS reveal a partial reduction of the core size of about 40% after 90 minutes at pH=3. Such scenario confirms the arrival of the nanoparticulate material in the small intestine. In the next step, the in vivo absorption through the small intestine by intestinal perfusion experiments is conducted using the sought nanoparticles in Wistar rats. The quantification of Fe in the NPs suspension before and after perfusion shows Fe absorption levels above 79%, never reported for other Fe treatments. Such high absorption levels do not seem to compromise cell viability, evaluated in enterocytes-like models (Caco-2 and HT-29) using cytotoxicity, ROS production, genotoxicity and lipid peroxidation tests. Moreover, regional differences in terms of Fe concentration are obtained among different parts of the small intestine as duodenum > jejunum > ileum. Complementary transmission electron microscopy (TEM) images show the presence of the intact particles around the intestinal microvilli without significant tissue damage. These studies show the high potential of these NP preparations for their use as oral management of anaemia.

SCHOLARONE™
Manuscripts

In vitro and in situ experiments to evaluate the biodistribution and cellular toxicity of ultrasmall iron oxide nanoparticles potentially used as oral iron supplements.

J. García Fernández,[a,c] D. Turiel,[a] J. Bettmer,[a] N. Jakubowski,[b] U. Panne,[b,c] , L. Rivas García[d] , J. Llopis[d], C. Sánchez González[d] and M. Montes-Bayón[a*]

[a] Department of Physical and Analytical Chemistry, Faculty of Chemistry, University of Oviedo, Julián Clavería 8, 33006 Oviedo, Spain

[b] BAM Federal Institute for Materials Research and Testing, Richard-Willstaetter Str. 11, 12489 Berlin, Germany

[c] Humboldt-University Berlin, School of Analytical Sciences Adlershof, Unter den Linden 6, 10099 Berlin, Germany

[d] Biomedical Research Centre, iMUDS, Institute of Nutrition and Food Technology "José Mataix", Department of Physiology, Faculty of Pharmacy, University of Granada, Campus Cartuja, 18071, Granada, Spain

*montesmaria@uniovi.es; Phone: +34-985103478

For Peer Review Only

Acknowledgements

Authors kindly acknowledge Dr. Marcos García-Ocaña from Biotechnology and Biomedical Analysis Unit at University of Oviedo for the cell culture and advice. Funding from FC-15-GRUPIN14-010 (Principado de Asturias), CTQ2016-80069-C2-1R and the Excellence Initiative of the German Research Foundation (DFG) are also acknowledged. DTF acknowledges the Ministerio de Ciencia y Educación for the grant FPU15/02415.

Abstract

Well-absorbed iron-based nanoparticulated materials are a promise for the oral management of iron deficient anaemia. In this work, a battery of *in vitro* and *in situ* experiments are combined for the evaluation of the uptake, distribution and toxicity of new synthesized ultrasmall (4 nm core) Fe_2O_3 nanoparticles coated with tartaric/adipic acid with potential to be used as oral Fe supplements. First, the *in vitro* simulated gastric acid solubility studies by TEM and HPLC-ICP-MS reveal a partial reduction of the core size of about 40% after 90 minutes at pH=3. Such scenario confirms the arrival of the nanoparticulate material in the small intestine. In the next step, the *in vivo* absorption through the small intestine by intestinal perfusion experiments is conducted using the sought nanoparticles in Wistar rats. The quantification of Fe in the NPs suspension before and after perfusion shows Fe absorption levels above 79%, never reported for other Fe treatments. Such high absorption levels do not seem to compromise cell viability, evaluated in enterocytes-like models (Caco-2 and HT-29) using cytotoxicity, ROS production, genotoxicity and lipid peroxidation tests. Moreover, regional differences in terms of Fe concentration are obtained among different parts of the small intestine as duodenum > jejunum > ileum. Complementary transmission electron microscopy (TEM) images show the presence of the intact particles around the intestinal microvilli without significant tissue damage. These studies show the high potential of these NP preparations for their use as oral management of anaemia.

Keywords: iron nanoparticles, anaemia, ICP-MS, *in vitro, in situ,* intestinal perfusion.

For Peer Review Only

Introduction

Iron deficiency anaemia is one of the most global diseases nowadays (Alleyne, Horne, and Miller 2008). The most extended way to help to overcome this pathology is based on oral iron supplementation. These preparations are mainly composed of ferrous salts showing relatively low iron bioavailability and increasing the risk of inflammation of the gut epithelium (Dostal et al. 2011). The high amount of soluble iron remaining in the intestinal lumen can induce the generation of free-radicals through Fenton chemistry with the consequent harmful effect of oxidative stress (Tolkien et al. 2015).

To overcome the existing limitations of these preparations, the development of alternative therapies based on the use of nanostructured Fe is an important trend in the management of Fe-deficient anaemia (Alphandéry 2019). Iron nanoparticles are currently used in intravenous formulations to treat severe cases of anaemia (Auerbach and Ballard 2010; Jahn et al. 2011). However, the possibility of using nanostructured Fe-supplements for oral administration is still an area subject to extensive investigations (Hilty et al. 2010; Pereira et al. 2014). Oral delivery is the most accepted drug administration route among the various delivery pathways because of its advantages: painlessness, easy self-administration, high patient compliance, and feasibility for outpatients. In this regard, it is known that particle size is crucial when designing a new nanodrug. Actually, it has been published that reducing the particle size in some iron compounds may result in an increasing bioavailability and therefore, an increment of the absorption level (Shang, Nienhaus, and Nienhaus 2014). Furthermore, size does not only determine the way of cellular uptake, but also the clearance mechanisms from the body (via kidneys for particles smaller than 10 nm and via mononuclear phagocyte system for larger particles in organs) (Bobo et al. 2016). Thus, some of the current efforts to find the ideal formulation are focused on mimicking the ferritin model to encapsulate iron in

For Peer Review Only

nanoparticulated form and releasing it with minimum side effects (Powell et al. 2014). Regarding the surface of the nanoparticulate material, a successful possibility includes the use of biocompatible ligands such as low-molecular-weight organic acids like tartaric or adipic acids. In this vein, iron nanoparticles of less than 5 nm (ultrasmall), with a ferrihydrite structure (as the one located inside the ferritin cage) have been synthesized and show a great potential in terms of anaemia correction (Hilty et al. 2010; Pereira et al. 2014) and will serve as the bases for this study. However, these preparations still need further investigation, especially in *ex vivo* and *in vivo* environment, where the characterization of nanoparticles is considered a challenge (Fernández et al. 2018).

Iron absorption takes place mainly at the apical membrane of duodenal enterocytes. The Caco-2 cell line is a well-established enterocyte model used for iron absorption and bioavailability studies at the cellular level (de Angelis and Turco 2011; Sambuy et al. 2005). On the other hand, the human adenocarcinoma cell line HT-29 is receiving special interest in studies focused on food digestion and bioavailability due to the ability to express characteristics of mature intestinal cells (Martínez-Maqueda, Miralles, and Recio 2015). Although the results obtained with human cells cannot be directly extrapolated to *in vivo* experiments, they offer a valuable opportunity to identify modifications that the nanodrug may suffer during absorption and these preliminary data will help to perform further *in vivo* studies in animal or humans. In any case, it is clear that the accurate intestinal permeability for drugs and nutrients is difficult to directly study in humans (Roos et al. 2017). Therefore, a number of *in vitro* and *in situ* experimental models have been developed, which determine the intestinal absorptive potential of a drug and the mechanism of absorption (S. Wang et al. 2014). Among these methods, the use single-pass intestinal perfusion (SPIP) experiments is the most frequently used technique, providing conditions closer to oral administration (Zakeri-Milani et al. 2007). This

For Peer Review Only

technique provides the unique advantages of experimental control (compound concentration and intestinal perfusion rate) and the ability to study regional differences; factors that may influence the intestinal absorption of a compound (Gamboa and Leong 2013). Thus, small intestine perfusion experiments seem to be particularly adequate to study NPs absorption in animal models (Sinnecker et al. 2014).

In this work, the aim is to characterize the fate and toxicological behaviour of ultrasmall tartaric and adipic acid-coated iron oxide nanoparticles (TA-FeNPs) using a battery of in vitro and in situ experiments. The first experiments are aimed to ensure that the particles remain stable within the gastro-intestinal track by evaluating their physicochemical behaviour in acidic environments using TEM and newly developed HPLC-ICP-MS strategies. Furthermore, intestinal absorption experiments by SPIP in combination with TEM and ICP-MS are conducted in animal models. The separation of the different regions of the small intestine should permit to establish the area where highest absorption has taken place. The toxicological aspects concerning the damage induced in enterocytes due to the NPs uptake is evaluated by addressing cell viability and ROS formation in cell Caco-2 and HT-29 cell models and correlated with the NPs absorption levels.

Experimental

Instrumentation

The determination of Fe in the different tissues was conducted by ICP-MS using an Agilent 7700 ICP-MS (Agilent Technologies, Santa Clara, CA), equipped with an octopole reaction system (ORS) and iCAP™ TQ ICP-MS (Thermo Fisher Scientific, Bremen, Germany). The ICP-MS instruments were fitted with a concentric nebulizer and a double pass spray chamber (in the Agilent 7500c system) and a cyclonic one (in the

For Peer Review Only

iCAP™ TQ ICP-MS). Hydrogen was employed as reaction gas to eliminate $^{40}Ar^{16}O^+$ and $^{40}Ar^{16}O^1H^+$ polyatomic interferences affecting ^{56}Fe and ^{57}Fe, respectively. Operating conditions are provided in Table S1.

Materials and Methods

Iron (III) chloride hexahydrate (98%, Sigma-Aldrich, Madrid, Spain) was used as nanoparticle precursor. Sodium tartrate dehydrated (99-101%, Sigma-Aldrich) and adipic acid (99%, Sigma-Aldrich) were solubilized in 0.9% sodium chloride (Merck, Darmstadt, Germany) solution and used as coating agents. Ammonium acetate (>98%, Sigma-Aldrich) was used for the synthesis buffer and 5 mol L^{-1} sodium hydroxide (Merck) was prepared for nanoparticle precipitation. All working standard solutions were prepared using 18 MΩ·cm de-ionized water obtained from a Milli-Q system (Millipore, Bedford, MA, USA).

Synthesis of nanoparticles. Iron nanoparticles were synthesized in the lab following a slightly modified protocol from Pereira et al. for the Fe-tartrate modified nanoparticles (Pereira et al. 2014).(Powell et al. 2014)(Powell et al. 2014)(Powell et al. 2014)(Powell et al. 2014) This method is based on the precipitation of Fe^{3+} in presence of highly basic medium (5 mol L^{-1} NaOH solution) with the addition of tartrate and adipic acid solution for the iron core coating as described somewhere else. The molar ratio tartaric: adipic: Fe used corresponds to 1:1:2, which has given best performance in previous experiments. The three components are mixed and constantly stirred in a buffer media (ammonium acetate 50 mmol L^{-1} at pH 4). The initial pH of the mixture is increased stepwise until reaching pH 8. When mixture turns dark brown/blackish, centrifugation and ultrafiltration (30,000 Da; 3,000 Da Ultra-15 MWCO centrifugal filter units, Millipore) steps are needed to separate the microparticulate and nanoparticulate iron

For Peer Review Only

fractions from the supernatant and remove excess of soluble ligands and the rest of reagents. Centrifuge Biofuge Stratos Heraeus (Thermo Scientific^{TM}) was used for these purposes. Size and shape characterization of the particles has been conducted by TEM, DLS and UV-VIS absorption spectra and is included as supplementary material (Figures S1, S2, S3 and S4).

*Simulation of digestion medium: acid lability assays***.** To evaluate the effect of the pH on the stability of the synthesized iron nanoparticles, similar conditions to these assayed in the protocol by Pereira et al. (Pereira et al. 2014) were taken. In brief, the freshly prepared TA-FeNPs suspended in 0.15 mol L^{-1} NaCl (to obtain a 2 mmol L^{-1} Fe concentration) were incubated for 95 minutes at room temperature. The pH was then lowered to pH 3.0 with 1 mol L^{-1} HCl and aliquots from these solutions were taken at different times (0, 5, 10, 15, 35, 55 and 95 minutes). To assess the fractionation of the iron into percentages of microparticulate, nanoparticulate and soluble iron during the process, centrifugation and ultrafiltration steps were applied. NPs suspensions were first centrifuged (10,000 g x 5 min) and the sediment (if present) was considered as the microparticulate fraction. In order to isolate the soluble iron and to distinguish it from the nanoparticulate form, the supernatant from the previous centrifugation was ultrafiltered (10,000 g x 10 min) using a cut off ultrafiltration through 3 kDa (Amicon® Ultra Centrifugal Filters, EMD Millipore, Darmstadt, Germany). The total iron was determined by ICP-MS and microparticulate, nanoparticulate and soluble fractions were expressed as percentage in relation to total iron content. The experiments have been conducted by triplicate. The evolution of the nanoparticulated fraction in terms of size and shape was studied by TEM and reversed phase HPLC-ICP-MS using the conditions published elsewhere (Fernández et al. 2018).

URL: http://mc.manuscriptcentral.com/tnan

For Peer Review Only

Intestinal perfusion experiments in animal models. This study was conducted in male Wistar rats weighing 182 ± 6 g (Charles River Laboratories, L'Arbresle, France) randomly divided into two groups: (a) four rats for the study of a control group and (b) four rats for the study of the absorption of FeNPs. The rat intestinal perfusion procedure was conducted following a method described previously (Zakeri-Milani et al. 2007). The small bowel has been selected for the study since it is widely known that most of the absorption of Fe occurs in the duodenum and upper part of the jejunum (O'Dell 1997). For this aim, twenty-four hour fasted rats were initially anaesthetized (1 mL/100 g of body weight, intraperitoneally solution of sodium thiopental 0.5% (m/V), Tiobarbital®, BBraun Vetcare, Spain) and kept under continuous anaesthesia during the entire perfusion. Then, after opening the abdominal cavity, the small intestine was exposed and an incision was made first at the pyloric sphincter and then at the ileocecal valve, and a catheter was inserted into the lumen via the incisions. After, the intestine contents were flushed by pumping of isotonic saline solution (37°C), the small intestine was continuously perfused with 20 mL of TA-FeNP containing solution (35.6 ± 0.6 $mg \cdot L^{-1}$ FeNPs in Tyrode solution) at a rate of 0.19 $mL \cdot min^{-1}$ at 37°C using a peristaltic pump. Composition of the perfusion solution was as follows: 8.0 $g \cdot L^{-1}$ NaCl, 0.2 $g \cdot L^{-1}$ KCl, 0.2 $g \cdot L^{-1}$ $CaCl_2$ anhydrous, 0.1 $g \cdot L^{-1}$ $MgCl_2$ anhydrous, 0.05 $g \cdot L^{-1}$ $NaH_2PO_4 \cdot H_2O$ and 1 $g \cdot L^{-1}$ glucose (pH 7). The experiment was performed in a thermoregulated chamber. The control group were perfused with Tyrode solution devoid of FeNP, in identical conditions to those described. After perfusion, the small intestine was extracted and its length and width were registered. Then, fractions of duodenum, jejunum and ileum were collected, as well as fractions of liver and kidney. All the organs were thoroughly washed with saline solution before digestion in order to eliminate the adsorbed Fe nanoparticles that could

URL: http://mc.manuscriptcentral.com/tnan

be potentially present. Additionally, aliquots of blood were drawn from the aorta by a heparinized syringe. All samples were frozen at −80 °C until further analysis.

The calculations for the absorption are given in equation [1] as reported by Escribano et al. (Escribano et al. 2012) :

$$[1] \qquad Permeability = \frac{f \times (C_{in} - C_{out})}{C_{out} \times 2\Pi \times r \times L}$$

Where C_{in} and C_{out} are the Fe concentrations of the influx and efflux normalized to the dimensions of the intestine (r: radius and L: length) and f is flow of the perfusion solution (0.2 mL min^{-1} in this case). All experiments were undertaken according to Directional Guides Related to Animal Housing and Care (European Community Council, 2010), and the Animal Experimentation Ethics Committee of the University of Granada approved all procedures.

Tissue samples preparation. Tissue samples were freeze-dried and digested using a microwave (Ethos 1, Milestone S.r.l., Italy). In brief, approximately 0.1 g of each lyophilized sample was placed into a polytetrafluoroethylene digestion vessel. Then, 5 mL of sub-boiling nitric acid and 3 mL of hydrogen peroxide (30%, Suprapur) were added and the digestion program was applied. A blank underwent in the same procedure. All the plastic containers used in the analysis were previously cleaned with sub-boiling nitric acid and ultra-pure water obtained using a Milli Q system (Millipore, Bedford, MA, USA). At the end of the digestion, the resulting solutions were made up to 50 mL with ultrapure water for further ICP-MS analysis. Iron total quantification was measured by collision cell ICP-MS (H_2 mode). Calibration curves were prepared following the addition of germanium as an internal standard, using stock solutions of 1000 mg L^{-1} (Merck). The mean of five independent replicates was used for determination of iron concentration. Obtained values were expressed as mg Fe·kg^{-1} of dried sample.

URL: http://mc.manuscriptcentral.com/tnan

For Peer Review Only

TEM images of tissues. Tissues samples were fixed with fresh primary fixative (1.5% glutaraldehyde, 1.0% formaldehyde in 0.05 mol L^{-1} sodium cacodylate buffer, pH 7.4) and post-fixed with secondary fixative (1% osmium tetroxide, 1% potassium ferrocyanide in Milli Q water) followed by dehydration with ascending series of alcohol before embedding samples in epoxy resin. Ultra-thin sections were cut and doubly stained with uranyl acetate and lead citrate. A transmission electron microscope LIBRA 120 PLUS microscope at 120 kV (Carl Zeiss SMT., Oberkochen, Germany) was used to determine the distribution and uptake of TA-FeNPs.

Cytotoxicity and ROS production. Caco-2 and HT-29 cells were cultivated at 37^{o}C in an atmosphere of 5% CO_2 and 95% air at a relative humidity of approximately 95%. Cells were maintained in T-75 flasks using Minimum Essential Medium (MEM, PAA Laboratories, Yeovil, UK) supplemented with 10% foetal bovine serum (FBS "Gold", PAA Laboratories), 1% penicillin/streptomycin and 1% fungizone (Invitrogen, Paisley, UK). The growth medium was changed every 2-3 days. MTT-Assay was carried out in order to assess cytotoxicity of synthesized FeNPs in the two lines. For this aim, cells grown in a 96-well flat bottom plate are incubated with different concentrations of FeNPs (0 to 4 mmol L^{-1}, in triplicate wells) for 48 h. The MTT reagent (3-(4,5-dimethylthiazol-2-yl)-2,5-diphenyltetrazolium bromide) is added and incubated for 2 h in a humidified atmosphere (37ºC, 5% CO_2, 95% humidity). After this incubation period, the formazan dye formed is quantified with a scanning multi-well spectrophotometer. The measured absorbance at appropriate wavelength (570 nm) directly correlates to the number of viable cells.

For the ROS production, Caco-2 cells were seeded at a density of $25 \cdot 10^3$ cells/well in a 96-well plate and incubated overnight to allow them to grow. The cells were incubated with TA-FeNPs and $FeSO_4$ at 0.25 mmol L^{-1} for 24 hours. ROS Assay kit

For Peer Review Only

(Bioquochem, Spain), uses 2'-7'dichlorofluorescin diacetate (DCFH-DA), a cell permeant reagent fluorogenic dye that measures hydroxyl, peroxyl and other ROS activity in the cell. After cell uptake, DCFH-DA is deacetylated by cellular esterases to a non-fluorescent compound, which is later oxidized by ROS into 2'-7'dichlorofluorescein (DCF). DCF is a fluorescent compound with a maximum excitation and emission spectra of 485 nm and 535 nm, respectively. Fluorescence was measured using a microplate reader (Infinitive 200, Tecan, Zürich, Switzerland). Tert-butyl hydroperoxide (TBHP) is employed as positive control. Results from both iron species ($FeSO_4$ and FeNPs) were corrected considering cell uptake studies.

Comet assay. The alkaline Comet assay was performed as previously described (Collins 2004). Briefly, $3x10^6$ HT-29 cells were analyzed per slide in 0.5% low melting point (LMP) agarose (Invitrogen). Slides were subjected to 1h lysis, 20 min denaturing at pH>13, and 20 min electrophoresis at 0,81V/cm and 300mA, at 4ºC in darkness. After neutralization and fixation, each slide, coded for blind analysis, was stained with 40µL ethidium bromide (0.4 µg/mL) and 1µL fluorescence protector Vectashield® (VECTOR laboratories, Inc. Burlingame). Nucleoids were visualized at 400x magnification with an OlympusBX61 fluorescence microscope, equipped with fluorescence filters and OlympusDP-70 CCD-coupled camera (at SCTs, University of Oviedo). Nucleoids from 50 cells/slide were scored and photographs were analyzed with Komet 5 (Kinetic Imaging Limited, UK). Three slides were analyzed per sample (control, exposed to TA-FeNPs at 0.25 mmol L^{-1} and positive control). The percentage of DNA in the tail was used to determinate the damage.

Lipids peroxidation assay. Malondialdehyde (MDA) can be generated by oxidizing agents like iron nanoparticles that alters lipid structure, creating lipid peroxides. MDA is measured as a adduct with thiobarbituric acid. The MDA-TBA adduct can be quantified

URL: http://mc.manuscriptcentral.com/tnan

For Peer Review Only

fluorometrically (Ex/Em = 532/553 nm) with a calibration curve in the range of 0 and 5 μM. This method, is adequate to determine the relative lipid peroxide content of samples, including cell culture supernatants. To conduct this assay, 4 x 10^5 cells (three independent cultures of control cell and cells exposed to TA-FeNPs at 0.25 mmol L^{-1}) were disrupted by ultrasonic treatment (ten cycles) and suspended in PBS buffer. The assay with the supernatant followed the protocol given by the manufacturers (Bioquochem, Asturias, Spain).

Statistical analysis. All variables and indexes were analyzed with descriptive statistics, and the results are reported as the mean and standard deviation. Statistical comparisons among the groups were performed by the Mann–Whitney test, a nonparametric testing for unrelated samples. All analyses were carried out with the version 20.0 of the Statistical Package for Social Sciences (SPSS Inc., Chicago, IL). Differences were considered significant at the 5% probability level. For the Comet assay, the statistical analysis was performed with the t-Student test.

Results

Simulation of digestion medium: acid lability assays.

The solubilisation of the synthetic TA-FeNPs was studied in a simulated digestion medium, using conditions taken from the literature (Pereira et al. 2014). The solubility of the TA-FeNPs was determined at pH 3.0 (corresponding to the lower end of the pH range of the postprandial gastric environment) at different times (different transit times). The different fractions (microparticulate, nanoparticulate and soluble Fe) were obtained as described in the procedures section and the Fe content measured by ICP-MS. The obtained results are shown in Figure 1A. As can be seen, the initial dissolution of the TA-FeNPs occurs within the first 10 minutes of mixing. Afterwards, minimum changes were

For Peer Review Only

detected during the remaining time of the experiment. Finally, after about 95 minutes, approximately 50% of the initial TA-FeNPs passed the filtration system (reducing its original diameter) under the working conditions. For evaluation of the size and morphology of the particles after incubation, TEM measurements of the higher and lower fractions of the ultrafiltrate material after acid treatment were taken. These data are shown in Figures 1B and C respectively. As can be seen there is a slight shift of the measured diameters of the nanoparticles towards smaller diameters in the case of the filtrate material (-3 kDa) which reveals minimum solubilisation. The same sample was also analysed by HPLC-ICP-MS with a previously optimized strategy for this particles (Fernández et al. 2018). Figure 2 shows the chromatograms before incubation and after 95 minutes of incubation at pH=3. Upon incubation, a double peak is observed in the chromatogram (black trace) revealing the coexistence of the original nanoparticles (blue trace, 5.3 minutes) and a smaller particle population eluting at longer retention times (5.8, black trace). Thus, is it possible that the labelled "soluble fraction" of Fig. 1 is ascribed to smaller size nanoparticles that are not retained during ultrafiltration confirming the results on total Fe determination and also those obtained by TEM. In any case, the presence of intact nanoparticles can be clearly seen confirming the lower degradation occurring due acidic incubation (pH=3). Such findings confirm the need for evaluation of the intestinal absorption of the intact preparation.

Intestinal perfusion studies: Iron absorption and distribution through the small intestine.

Iron absorption in the small intestine was carried out by intestinal perfusion of the TA-FeNPs suspensions in anaesthetized animals. For this purpose, the animals were treated as described in the procedures section. The iron concentration was measured by ICP-MS after adequate dilution in the infused solution before and after perfusion.

URL: http://mc.manuscriptcentral.com/tnan

For Peer Review Only

The obtained results (before and after normalization by the dimensions of the intestine of the different animals) are shown in Table 1. As can be observed in the table, the permeability for these NPs is approximately 8 cm min^{-1}. Calculated as percentage, it can be seen that the Fe absorption is above the 79% (see Table 1), which is one of the highest values ever reported for iron preparations. The differential absorption of TA-FeNP in the different segments of the intestine, and considering that the main route of absorption is transcellular, the Fe content was quantified in the three intestinal segments (duodenum, jejunum and ileum) of perfused rats against control rats. The tissues were also used to obtain TEM images in the search for intact NPs. Figure 3 shows the total iron concentration in duodenum, jejunum and ileum after perfusion experiments in respect to the respective controls. As can be seen in the figure, control animals (perfused with tyrode solution devoid of FeNPs) show similar iron levels in the three regions of the small intestine (concentrations are between 32 ± 16 $mg·kg^{-1}$ in the duodenum and 29 ± 12 $mg·kg^{-1}$ in the ileum). However, the animals perfused with the FeNPs solution (35.6 mg L^{-1} as Fe) show a significantly higher Fe accumulation in the duodenum, which is a factor of 5-fold with respect to the control, followed by the jejunum (about 3-fold) and finally ileum (2-fold). These results are statistically different in duodenum and jejunum ($p<0.01$) and slightly different in the case of ileum ($p<0.05$).

The TEM images of the ileum of one of the treated rats can be seen in Figure 4A in comparison to the same tissue of the control animal (Figure 4B). The presence of TA-FeNPs into the enterocytes as well as the absence of histological damage in the tissues can be observed. TEM studies show also the absence of histological damage in the three sections of the small intestine, duodenum, jejunum and ileum (see Fig S5, S6 and S7). The measurement of the particle diameter revealed sizes of about 3 nm, in accordance with the initial size of the TA-FeNPs.

URL: http://mc.manuscriptcentral.com/tnan

For Peer Review Only

Toxicity of the TA-FeNPs in enterocytes-like cell models: viability and ROS production.

Since no histological damage was observed in the exposed tissues, the potential toxicity of taken up NPs in Caco-2 cell monolayers and HT-29 enterocytes-like cell models was conducted. Viability assays were accomplished using concentration levels of TA-FeNPs (up to 4 mmol L^{-1}) and long exposure time (48 h). The concentration selected for the perfusion experiments (230 mg Fe / day for an adult, which equals 20 ml of a solution of 35 mg FeNP / L or 0.62 mmol L^{-1}) fits within the pharmacological dose of iron currently recommended in clinics (40 to 300 mg Fe / day for adults). Thus, the concentrations for the in vitro experiments were also selected within that range. Results of the MTT assay are shown in Figure 5. In this range of concentrations of TA-FeNPs, considered within therapeutic levels, no cytotoxicity has been observed in Caco-2 or HT-29. Viability values above the 100% are achieved, suggesting a positive effect of the nanoparticles on the enzymatic activity. However, cell damage cannot be completely discarded, since the cell has repair mechanisms that the MTT assay cannot detect. The results are statistically significant in respect to the control samples for the Caco-2 model. The differences observed between the two cell lines might be attributed to the fact that Caco-2 shows an ease of access of highly diffusible small molecules to the microvilli, due to an almost complete lack of mucus (Nollevaux et al. 2006).

For addressing the effect of the TA-FeNPs on the ROS production in Caco-2 cell model, the fluorescence of DCFH-DA, a cell permeating fluorogenic dye that measures hydroxyl, peroxyl and other ROS activity in the cell was used. As can be seen in Figure 6A, the cellular DCFDA assay revealed the evidence of reactive oxygen species generation with time after incubating with both, TA-FeNPs and $FeSO_4$ at 0.25 mmol L^{-1} Fe, in agreement with the expected for iron compounds (B. Wang et al. 2013). A concentration of 0.25 mmol L^{-1} was chosen attending to a normal dose that a patient with

URL: http://mc.manuscriptcentral.com/tnan

For Peer Review Only

anaemia would receive (Alleyne, Horne, and Miller 2008). The fluorescence intensity increases with time in both cases and duplicates the background values from the cell control. However, it can be noticed that cellular oxidative stress is not higher than the observed for $FeSO_4$ exposure (conventionally used for anaemia treatment). It has to be noticed that the data have been corrected by the cellular Fe uptake in both models, which is significantly higher in the case of the NPs. In any case, the TA-FeNPs produce significantly lower oxidative damage than the positive control ($p<0.01$) and comparable or even lower to the level induced by $FeSO_4$, regularly used in the treatment of anaemia.

Genotoxic damage was assessed by the Comet assay using the same concentration of nanoparticles than in the case of the ROS production assay (0.25 mmol L^{-1}). The obtained results are shown in Figure 6B where the % of the tail is represented for the three treatments. Statistical analysis using t-student test (p>95%) revealed not significant differences between the control and the treated cells but statistically significant results with respect to the positive control (treated with H_2O_2).

Finally, lipids peroxidation assay was also evaluated to address the stability of the cellular membrane upon exposure to TA-FeNPs.

Iron transport and distribution in other tissues.

As a first step to address the translocation of TA-FeNPs once they are absorbed in the small intestine, different tissues samples were collected for Fe determination after perfusion. Some of these organs are kidney and liver. Total iron analysis in these organs as well as in whole blood are collected in Table 2. The obtained results reveal that kidney and blood show an increment of 16 and 15% respectively, in comparison to their corresponding control samples (can be significant considering the dilution that the particles undergo when reaching the vascular system). In contrast, Fe concentration in liver samples levels remain stable and no significant variation can be found after 100

For Peer Review Only

minutes TA-FeNPs perfusion. These results are in good agreement with the expected for these small size nanoparticles (Arruebo et al. 2007). However, due to the small size of TA-FeNPs that allows glomerular filtration, a significant increase in renal iron levels has been detected.

Some of these tissues, e.g. blood, spleen, kidney and liver, were also fixated as previously described, to be studied by TEM. Results can be seen in Figure 7, in which the TA-FeNPs can be observed in blood (Fig. 7a) and allocated in macrophages digestive vacuoles in small associations of the spleen (Fig. 7b), contributing to the biological digestion and liberation of iron from the nanoparticle originally administered. Although the results of total Fe in the liver do not show significant differences with respect to the control, the TEM images shows the undeniable presence of the particles in kidney (glomerulus, Fig. S8) and liver (disse space, Fig. S9). Therefore, both techniques are necessary to track the presence of particles in the different biological compartments.

Discussion

The investigation of in vivo NP intestinal uptake after oral exposure is influenced by factors such as dietary status, mucosal secretions, variability in gastric and intestinal pH or gastrointestinal transit time. In this regard, the potential solubilisation of the TA-FeNPs under study before reaching the small intestine (e.g. due to pH variation) has been addressed since the Fe absorption will depend on the size and shape of the nanoparticulated material that will eventually reach this organ. The results revealed that after about 10 minutes approximately 50% of the initial nanoparticulated fraction remains unchanged while other 50% evolves to smaller sized particles or ionic Fe. These results are in good agreement with previously published work using similar nanoparticles and different methodologies (Pereira et al. 2014). In this work, the complementary use of

For Peer Review Only

TEM permitted to address the presence of smaller particles in respect to the original size (40%) that was further confirmed by HPLC-ICP-MS. The latter technique has proved to be an invaluable tool for this type of research, particularly in the case of Au and Ag NPs in biological tissues and fluids (Lopez-Chaves et al. 2018). In this specific case, the observed results confirmed, once again, the presence of two nanoparticulated fractions of approximately similar abundance after incubation for 95 min at pH=3 corresponding to the original particles and to smaller sized particles respectively.

Therefore, it could be expected that once administrated orally, these TA-FeNPs present certain stability in that digestive tract with minor size changes and negligible shape alterations. Such behaviour is possibly associated to the acid coating containing tartaric and adipic acid which serves to stabilize the structure. These behaviour to what has been observed in other commercial Fe-oxide NPs containing, for instance, sucrose as coating material which exhibited rapid and quantitative solubilisation in physiological media (up to 90% in less than one hour) (García-Fernández et al. 2017).

Regarding the quantitative iron absorption experiments in the small intestine, among the permeability models available to study transepithelial transport, the *in situ* intestinal perfusion technique seems an appropriate approach when specific absorption is under evaluation. Its advantage is to provide an intact blood supply and a functional intestinal barrier allowing the study of the influence of transporters in absorption. Using this model, the Fe absorption from the TA-FeNPs turned out to be above of 79%, among the highest ever reported for Fe. Literature results of iron absorption in animal models showed values ranging from 10 to 60% depending on various factors when the given chemical form was ferric citrate (Pallarés et al. 1993; Sanchez-Morito et al. 2000; Sánchez-González et al. 2014). In addition, a study of intestinal perfusion carried out using ferric citrate under similar set of conditions revealed a percentage of absorption in

URL: http://mc.manuscriptcentral.com/tnan

For Peer Review Only

the duodenum lower than that observed the present study (about 30%) (Gómez-Ayala et al. 1997). Concerning nanoparticulate material, it has been reported that in rodents the intestinal uptake levels of NPs range from 2 to 34% depending on the particle size (from 20 to 200 nm), dosages, application protocols and detection regimes (Sinnecker et al. 2014). In the actual experiments, the ultrasmall TA-FeNPs (3.7 nm core size and about 11 nm hydrodynamic diameter) might favour their permeation into the enterocytes obtaining results on the upper level of this range. However, no data could be found of such small particle size to compare with the obtained results. With regard to the different intestinal regions involved in the absorption of the nanoparticulated material, the results revealed significant differences according to the sequence duodenum>jejunum>ileum. Such results are in agreement with the published literature that confirms highest elemental iron absorption in the duodenum and upper part of the jejunum for other iron species (Gulec, Anderson, and Collins 2014). Here, the determining role of duodenum in the absorption of nanoparticulated Fe is evident and has never reported before for this kind of NPs.

The stability and low dissolution of the particles could be also confirmed by TEM measurements of the different tissues revealing sizes of about 3 nm, in accordance with the initial size of the TA-FeNPs which shows the relatively low dissolution of these particles during the perfusion experiments and the absence of agglomerates of nanoparticles in the intestinal lumen and the intestinal barrier. This is highly interesting since hundreds of Fe atoms are safely packed into a nanoscaled iron oxide/hydroxide cores resulting in less oxidative stress and less side effects. In any case, tissue integrity evaluated after the experiment by histological examination was found to be in an acceptable range (Fig 3, S5, S6 and S7) with villi and enterocytes remaining intact after the perfusion, both in experiments with and without NP administration.

For Peer Review Only

Although no tissue damage was observed, the potential intracellular toxicity caused by such a high cellular uptake was explored in Caco-2 cell monolayers, used as *in vitro* model since they have enterocyte-like characteristics as microvilli, tight junctions and duodenal transport systems and in HT-29 models. In addition, since Fe is a strong Fenton element, the possible damage ascribed to the production of excessive reactive oxygen species (ROS) was also evaluated. High ROS levels are indicative of oxidative stress and can damage cells by peroxidising lipids, altering proteins, disrupting DNA, interfering with signalling functions and modulating gene transcription. Cellular cytotoxicity was negligible even at highest concentrations and ROS production was comparable to this obtained by treating the cells with an inorganic Fe source ($FeSO_4$) once the values are normalized to the Fe uptake level. Such results correlate with previous studies conducted with these NPs that revealed a relatively low dissolution (and production of ionic iron species) in the cell cytosol beside the high uptake levels. This points out, once more, the efficacy of the particles to enter cells and the slow/controlled release of Fe that is desirable for the nanopreparations.

On the light of the observed results, the systemic drug delivery of these NPs seems to occur by transcytosis (mechanism by which NPs are internalized by endocytosis through the apical pole of the cell membrane and further released by exocytosis into the interstitial space through the basolateral pole). It has also been described that, alternatively, macromolecules may be absorbed via the paracellular pathway crossing the "tight junction" barrier between cells and diffuse into the intercellular space. In both cases the TA-FeNPs would access the portal vessels by which they will be conducted from the gastrointestinal tract to the liver. In this vein, the mobilization experiments (by ICP-MS + TEM) showed that after 100 minutes perfusion, the TA-FeNPs are transferred across the basolateral membrane (BLM) due to their small diameter. Then, they are systemic

For Peer Review Only

distributed as revealed by their presence in blood and other organs, like spleen. Due to their size and stability, these nanostructures have probably passed the physiological barriers and reach the blood stream almost unmodified. Although their presence in the blood stream might be also explained as aggregation of dissolved Fe, this is unlikely to occur due to the presence of serum proteins like transferrin and the high affinity of Fe for this molecule (K_f=10^{10}). Even in a high excess of Fe, other complexes (NTBI, non-transferrin bound Fe) can be also form avoiding the formation of nanoparticles. (Ganz and Nemeth 2011; Porter et al. 1996).

Once in the organs, the slowly dissolving ionic iron delivered progressively from the TA-FeNPs could potentially be incorporate into ferritin in the enterocyte, liver, spleen and bone marrow, as described before (Turiel-Fernández, Bettmer, and Montes-Bayón 2018). Finally, the TA-FeNPs seem to be excreted via renal glomerular filtration, as significantly increased Fe levels have been detected in kidney tissues. This finding agrees with other publications describing that smaller NPs are subject to rapid renal elimination, while larger ones that cannot pass through the filtration membrane, remain in the liver, spleen, and bone marrow (Mornet et al. 2004). All these finding confirm a high stability of this specific nanoparticles, a rapid absorption and transport in the body and a regulated incorporation into the organs. Their rapid renal excretion reduces the possibility of iron overload.

Conclusions

Ultrasmall TA-FeNPs have proved to be an interesting alternative for the oral treatment of iron deficiency anaemia. This specific nanocompound of less than 4 nm of diameter size, is based on ferrihydrite core surrounded by a tartrate-adipate coating. Stability at low pH, simulating gastric conditions, was evaluated showing that unlike most iron

URL: http://mc.manuscriptcentral.com/tnan

For Peer Review Only

complexes, TA-FeNPs are not totally solubilized in acid medium and the nanostructure remains despite the drastic changes in pH.

The in situ studies accomplished by small intestine perfusion experiments showed an absorption up to 79.3%, proving the effectiveness of the FeNPs. Moreover, important role of duodenum in the iron absorption was also shown with up to 38% and 62% more iron uptake in this region than jejunum and ileum, respectively. Beside such high uptake, the low cytotoxicity and ROS production detected revealed small increments in the generation of free radicals, probably related to the slow dissolution of the iron from the nanoparticles. In this sense, the oxidative stress effect caused by the FeNPs is lower than this generated by $FeSO_4$, considering the lower absorption degree that this form of iron presents compared to the nanoparticulate preparation.

Regarding TA-FeNPs transport, the TEM results showed that bloodstream is involved in the systemic biodistribution of FeNPs to organs like spleen, liver and kidney. In summary, several obstacles typical of the oral delivery systems such as the mucus lining of the gastrointestinal tract or the variable acidic pH throughout the gastric system have been approached and overcome by facing TA-FeNPs to different in vitro and in situ models. These results might represent an additional piece of knowledge in the elucidation of TA-NPs metabolism.

For Peer Review Only

References

Alleyne, Michael, McDonald K. Horne, and Jeffery L. Miller. 2008. "Individualized Treatment for Iron-Deficiency Anemia in Adults." *American Journal of Medicine*. https://doi.org/10.1016/j.amjmed.2008.07.012.

Alphandéry, Edouard. 2019. "Biodistribution and Targeting Properties of Iron Oxide Nanoparticles for Treatments of Cancer and Iron Anemia Disease." *Nanotoxicology*. https://doi.org/10.1080/17435390.2019.1572809.

Angelis, Isabella de, and Laura Turco. 2011. "Caco-2 Cells as a Model for Intestinal Absorption." *Current Protocols in Toxicology*. https://doi.org/10.1002/0471140856.tx2006s47.

URL: http://mc.manuscriptcentral.com/tnan

Arruebo, Manuel, Rodrigo Fernández-Pacheco, M. Ricardo Ibarra, and Jesús Santamaría. 2007. "Magnetic Nanoparticles for Drug Delivery." *Nano Today*. https://doi.org/10.1016/S1748-0132(07)70084-1.

Auerbach, Michael, and Harold Ballard. 2010. "Clinical Use of Intravenous Iron: Administration, Efficacy, and Safety." *Hematology / the Education Program of the American Society of Hematology. American Society of Hematology. Education Program*. https://doi.org/10.1182/asheducation-2010.1.338.

Bobo, Daniel, Kye J. Robinson, Jiaul Islam, Kristofer J. Thurecht, and Simon R. Corrie. 2016. "Nanoparticle-Based Medicines: A Review of FDA-Approved Materials and Clinical Trials to Date." *Pharmaceutical Research*. https://doi.org/10.1007/s11095-016-1958-5.

Collins, Andrew. 2004. "The Comet Assay for DNA Damage and Repair." *Molecular Biotechnology*.

Dostal, Alexandra, Christophe Chassard, Florentine M. Hilty, Michael B. Zimmermann, Tanja Jaeggi, Samuela Rossi, and Christophe Lacroix. 2011. "Iron Depletion and Repletion with Ferrous Sulfate or Electrolytic Iron Modifies the Composition and Metabolic Activity of the Gut Microbiota in Rats." *The Journal of Nutrition*. https://doi.org/10.3945/jn.111.148643.

Escribano, Elvira, Xavier García Sala, Jorge Salamanca, Claudia Roig Navarro, and Josep Queralt Regué. 2012. "Single-Pass Intestinal Perfusion to Establish the Intestinal Permeability of Model Drugs in Mouse." *International Journal of Pharmaceutics*. https://doi.org/10.1016/j.ijpharm.2012.07.010.

Fernández, J. García, C. Sánchez-González, J. Bettmer, J. Llopis, N. Jakubowski, U. Panne, and M. Montes-Bayón. 2018. "Quantitative Assessment of the Metabolic Products of Iron Oxide Nanoparticles to Be Used as Iron Supplements in Cell Cultures." *Analytica Chimica Acta*. https://doi.org/10.1016/j.aca.2018.08.003.

Gamboa, Jennifer M., and Kam W. Leong. 2013. "In Vitro and in Vivo Models for the Study of Oral Delivery of Nanoparticles." *Advanced Drug Delivery Reviews*. https://doi.org/10.1016/j.addr.2013.01.003.

Ganz, Tomas, and Elizabeta Nemeth. 2011. "Hepcidin and Disorders of Iron Metabolism." *Annual Review of Medicine*. https://doi.org/10.1146/annurev-med-050109-142444.

García-Fernández, Jenifer, Jörg Bettmer, Norbert Jakubowski, Ulrich Panne, Elena Añón, María Montes-Bayón, and Alfredo Sanz-Medel. 2017. "The Fate of Iron Nanoparticles Used for Treatment of Iron Deficiency in Blood Using Mass-Spectrometry Based Strategies." *Microchimica Acta*. https://doi.org/10.1007/s00604-017-2388-8.

Gómez-Ayala, Adela E., Margarita S. Campos, Inmaculada López-Aliaga, Isabel Pallarés, Sanae Hartiti, Mercedes Barrionuevo, María J.M. Alférez, María C. Rodríguez-Matas, and Francisco Lisbona. 1997. "Effect of Source of Iron on Duodenal Absorption of Iron, Calcium, Phosphorus, Magnesium, Copper and Zinc in Rats with Ferropoenic Anaemia." *International Journal for Vitamin and Nutrition Research*.

Gulec, Sukru, Gregory J. Anderson, and James F. Collins. 2014. "Mechanistic and Regulatory Aspects of Intestinal Iron Absorption." *American Journal of Physiology-Gastrointestinal and Liver Physiology*. https://doi.org/10.1152/ajpgi.00348.2013.

Hilty, Florentine M., Myrtha Arnold, Monika Hilbe, Alexandra Teleki, Jesper T.N. Knijnenburg, Felix Ehrensperger, Richard F. Hurrell, Sotiris E. Pratsinis, Wolfgang Langhans, and Michael B. Zimmermann. 2010. "Iron from Nanocompounds Containing Iron and Zinc Is Highly Bioavailable in Rats without Tissue Accumulation." *Nature Nanotechnology*. https://doi.org/10.1038/nnano.2010.79.

Jahn, Markus R., Hans B. Andreasen, Sören Fütterer, Thomas Nawroth, Volker Schünemann, Ute Kolb, Wolfgang Hofmeister, et al. 2011. "A Comparative Study of the Physicochemical Properties of Iron Isomaltoside 1000 (Monofer®), a New Intravenous Iron Preparation and Its Clinical Implications." *European Journal of Pharmaceutics and Biopharmaceutics*. https://doi.org/10.1016/j.ejpb.2011.03.016.

Lopez-Chaves, Carlos, Juan Soto-Alvaredo, Maria Montes-Bayon, Jörg Bettmer, Juan Llopis, and Cristina Sanchez-Gonzalez. 2018. "Gold Nanoparticles: Distribution, Bioaccumulation and Toxicity. In Vitro and in Vivo Studies." *Nanomedicine:*

For Peer Review Only

Nanotechnology, Biology, and Medicine. https://doi.org/10.1016/j.nano.2017.08.011.
Martínez-Maqueda, Daniel, Beatriz Miralles, and Isidra Recio. 2015. “HT29 Cell Line.” In *The Impact of Food Bioactives on Health: In Vitro and Ex Vivo Models*. https://doi.org/10.1007/978-3-319-16104-4_11.
Mornet, Stéphane, Sébastien Vasseur, Fabien Grasset, and Etienne Duguet. 2004. “Magnetic Nanoparticle Design for Medical Diagnosis and Therapy.” *Journal of Materials Chemistry*. https://doi.org/10.1039/b402025a.
Nollevaux, Géraldine, Christelle Devillé, Benaïssa El Moualij, Willy Zorzi, Patricia Deloyer, Yves Jacques Schneider, Olivier Peulen, and Guy Dandrifosse. 2006. “Development of a Serum-Free Co-Culture of Human Intestinal Epithelium Cell-Lines (Caco-2/HT29-5M21).” *BMC Cell Biology*. https://doi.org/10.1186/1471-2121-7-20.
O’Dell, Boyd L. 1997. *Handbook of Nutritionally Essential Minerals Elements*. New York: Maecel Dekker.
Pallarés, I., F. Lisbona, I. Lopez Aliaga, M. Barrionuevo, M. J. M. Alférez, and M. S. Campos. 1993. “Effect of Iron Deficiency on the Digestive Utilization of Iron, Phosphorus, Calcium and Magnesium in Rats.” *British Journal of Nutrition*. https://doi.org/10.1079/bjn19930152.
Pereira, Dora I.A., Sylvaine F.A. Bruggraber, Nuno Faria, Lynsey K. Poots, Mani A. Tagmount, Mohamad F. Aslam, David M. Frazer, Chris D. Vulpe, Gregory J. Anderson, and Jonathan J. Powell. 2014. “Nanoparticulate Iron(III) Oxo-Hydroxide Delivers Safe Iron That Is Well Absorbed and Utilised in Humans.” *Nanomedicine: Nanotechnology, Biology, and Medicine*. https://doi.org/10.1016/j.nano.2014.06.012.
Porter, J. B., R. D. Abeysinghe, L. Marshall, R. C. Hider, and S. Singh. 1996. “Kinetics of Removal and Reappearance of Non-Transferrin-Bound Plasma Iron with Deferoxamine Therapy.” *Blood*. https://doi.org/10.1182/blood.v88.2.705.bloodjournal882705.
Powell, Jonathan J., Sylvaine F.A. Bruggraber, Nuno Faria, Lynsey K. Poots, Nicole Hondow, Timothy J. Pennycook, Gladys O. Latunde-Dada, Robert J. Simpson, Andy P. Brown, and Dora I.A. Pereira. 2014. “A Nano-Disperse Ferritin-Core Mimetic That Efficiently Corrects Anemia without Luminal Iron Redox Activity.” *Nanomedicine: Nanotechnology, Biology, and Medicine*. https://doi.org/10.1016/j.nano.2013.12.011.
Roos, Carl, David Dahlgren, Staffan Berg, Jan Westergren, Bertil Abrahamsson, Christer Tannergren, Erik Sjögren, and Hans Lennernäs. 2017. “In Vivo Mechanisms of Intestinal Drug Absorption from Aprepitant Nanoformulations.” *Molecular Pharmaceutics*. https://doi.org/10.1021/acs.molpharmaceut.7b00294.
Sambuy, Y., I. De Angelis, G. Ranaldi, M. L. Scarino, A. Stammati, and F. Zucco. 2005. “The Caco-2 Cell Line as a Model of the Intestinal Barrier: Influence of Cell and Culture-Related Factors on Caco-2 Cell Functional Characteristics.” *Cell Biology and Toxicology*. https://doi.org/10.1007/s10565-005-0085-6.
Sánchez-González, Cristina, Carlos López-Chaves, Cristina E. Trenzado, Pilar Aranda, María López-Jurado, Jorge Gómez-Aracena, María Montes-Bayón, Alfredo Sanz-Medel, and Juan Llopis. 2014. “Changes in Iron Metabolism and Oxidative Status in STZ-Induced Diabetic Rats Treated with Bis(Maltolato) Oxovanadium (IV) as an Antidiabetic Agent.” *The Scientific World Journal*. https://doi.org/10.1155/2014/706074.
Sanchez-Morito, N., E. Planells, P. Aranda, and J. Llopis. 2000. “Influence of Magnesium Deficiency on the Bioavailability and Tissue Distribution of Iron in the Rat.” *Journal of Nutritional Biochemistry*. https://doi.org/10.1016/S0955-2863(99)00076-5.
Shang, Li, Karin Nienhaus, and Gerd U. Nienhaus. 2014. “Engineered Nanoparticles Interacting with Cells: Size Matters.” *Journal of Nanobiotechnology*. https://doi.org/10.1186/1477-3155-12-5.
Sinnecker, Heike, Thorsten Krause, Sabine Koelling, Ingmar Lautenschläger, and Andreas Frey. 2014. “The Gut Wall Provides an Effective Barrier against Nanoparticle Uptake.” *Beilstein Journal of Nanotechnology*. https://doi.org/10.3762/bjnano.5.218.
Tolkien, Zoe, Lynne Stecher, Adrian P. Mander, Dora I.A. Pereira, and Jonathan J. Powell. 2015. “Ferrous Sulfate Supplementation Causes Significant Gastrointestinal Side-Effects in Adults: A Systematic Review and Meta-Analysis.” *PLoS ONE*.

For Peer Review Only

https://doi.org/10.1371/journal.pone.0117383.

Turiel-Fernández, Daniel, Jörg Bettmer, and Maria Montes-Bayón. 2018. "Evaluation of the Uptake, Storage and Cell Effects of Nano-Iron in Enterocyte-like Cell Models." *Journal of Trace Elements in Medicine and Biology*. https://doi.org/10.1016/j.jtemb.2018.05.002.

Wang, Bing, Jun Jie Yin, Xiaoyan Zhou, Ibrahim Kurash, Zhifang Chai, Yuliang Zhao, and Weiyue Feng. 2013. "Physicochemical Origin for Free Radical Generation of Iron Oxide Nanoparticles in Biomicroenvironment: Catalytic Activities Mediated by Surface Chemical States." *Journal of Physical Chemistry C*. https://doi.org/10.1021/jp3101392.

Wang, Shu, Rui Su, Shufang Nie, Ming Sun, Jia Zhang, Dayong Wu, and Naima Moustaid-Moussa. 2014. "Application of Nanotechnology in Improving Bioavailability and Bioactivity of Diet-Derived Phytochemicals." *Journal of Nutritional Biochemistry*. https://doi.org/10.1016/j.jnutbio.2013.10.002.

Zakeri-Milani, Parvin, Hadi Valizadeh, Hosnieh Tajerzadeh, Yadollah Azarmi, Ziba Islambolchilar, Saeed Barzegar, and Mohammad Barzegar-Jalali. 2007. "Predicting Human Intestinal Permeability Using Single-Pass Intestinal Perfusion to Rat." *Journal of Pharmacy and Pharmaceutical Sciences*.

For Peer Review Only

Table 1. Results obtained for the perfusion experiments in Wistar rats (n=4).

Compound	Perfused Fe ($mg \cdot L^{-1}$)	Absorbed Fe ($mg \cdot L^{-1}$)	% Absorption	Permeability ($cm \cdot min^{-1}$)
Control	0.004 ± 0.003	-	-	-
TA-FeNPs	35.6 ± 0.6	28.2 ± 2.1	79.3 ± 6.1	8.5 ± 0.8

Table 2. Iron content and increments in tissues of control (n=3) and perfused with TA-FeNPs group (n=3).

	Total iron content in control rats ($mg \cdot kg^{-1}$)	Total iron content in TA-FeNPs perfused rats ($mg \cdot kg^{-1}$)	Increment of iron (%)
Kidney*	47.87 ± 5.36	57.26 ± 7.11	16.4
Liver**	110.80 ± 17.22	109.67 ± 26.62	-
Blood***	289.34 ± 17.09	340.10 ± 11.44	14.9

*P<0.05; **No; ***P<0.001

For Peer Review Only

FIGURE CAPTIONS

Figure 1. A) Acid lability assay of TA-FeNPs at pH 3 showing the solubilization with time (nanoparticulate fraction is showed in pale blue bars; soluble fraction is represented in dark blue bars); B) TEM image and histogram of the diameters observed in the fraction >3KDa and C) TEM image and histogram of the diameters of the fraction <3KDa, both obtained after 95 min of acid incubation.

Figure 2. Chromatogram on the evolution of TA-FeNPs upon incubation at pH=3 for 95 minutes obtained by reversed phase HPLC (in presence of SDS) with ICP-MS detection (^{56}Fe). Original particles (blue trace) and particles after incubation (black trace). The inset correspond to the TEM images of the two set of particles.

Figure 3. Total Fe concentration levels in duodenum, jejunum and ileum of control rats (pale blue bars, n=4) and TA-FeNPs intestinal perfused rats (dark blue bars, n=4)

Figure 4. A) Transmission electron microscopy (TEM) images of the intestinal histology of ileum and the presence of FeNP (see yellow arrows) and B) same tissue for a control animal.

Figure 5. Cell viability in HT-29 (dark blue bars) and Caco-2 (light blue bars) after 48 h of TA-FeNPs exposure from 0-4000 µmol L^{-1} of Fe concentration.

Figure 6. A) ROS assay comparing the exposure of Caco-2 cells to TA-FeNPs vs $FeSO_4$. Tert-butyl hydroperoxide (TBHP) was used as positive control and controls of FeNPs, $FeSO_4$ and cells were used to establish background levels of fluorescence intensity. (a) vs 0; (b) vs 5; (c) vs 15; (d) vs 30; (e) vs 45; (f) vs 60; (g) vs 75; (*) cells+0.25mM NPs vs cells+0.25mM FeSO4; P<=0.05 in all cases; (n=3) B) results of the Comet assay expressed as % tail moment and cells images for control (I), TA-FeNPs exposed cells (II) and positive control (III); C) Lipid peroxidation assay by measurement of malondialdehyde production in control (pale grey) and TA-FeNPs treated cells (dark grey).

Figure 7. TEM images of previously fixed samples of a) blood and b) spleen (inset showing elemental analysis by EDX.

URL: http://mc.manuscriptcentral.com/tnan

For Peer Review Only

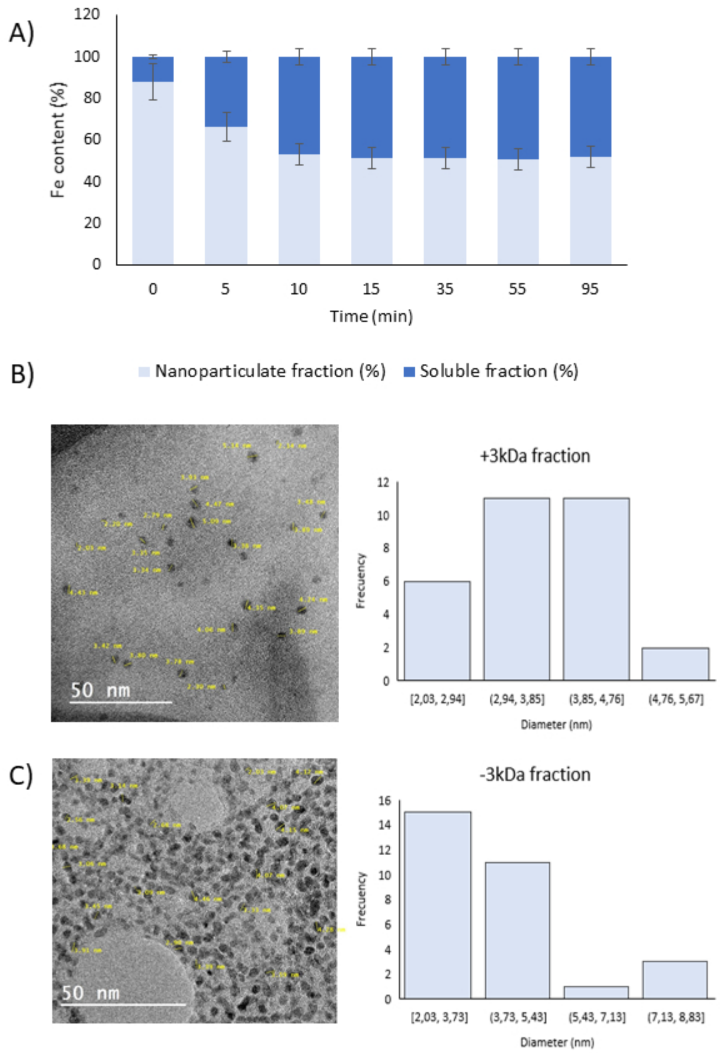

Figure 1

Figure 1

190x254mm (96 x 96 DPI)

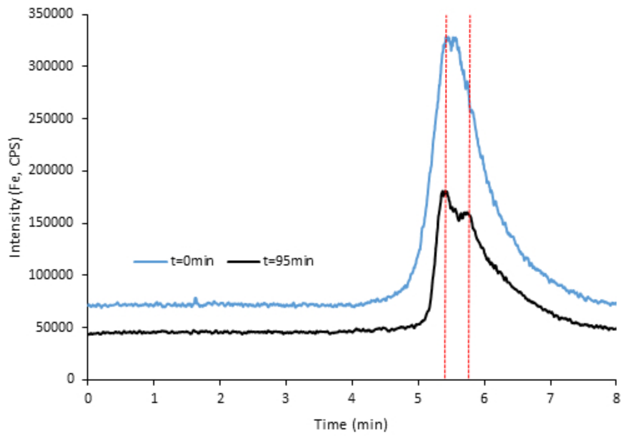

Figure 2

Figure 2

190x254mm (96 x 96 DPI)

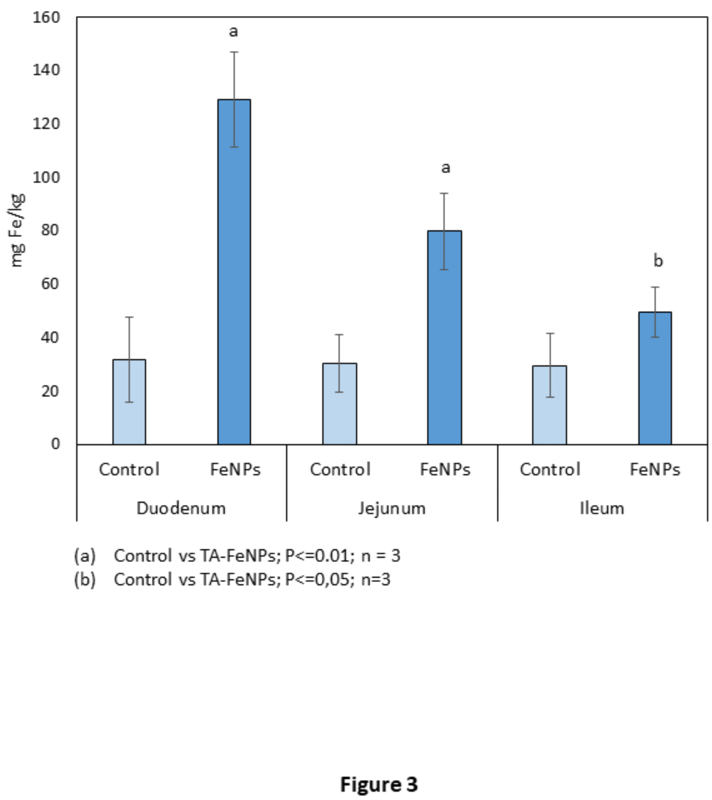

Figure 3

190x254mm (96 x 96 DPI)

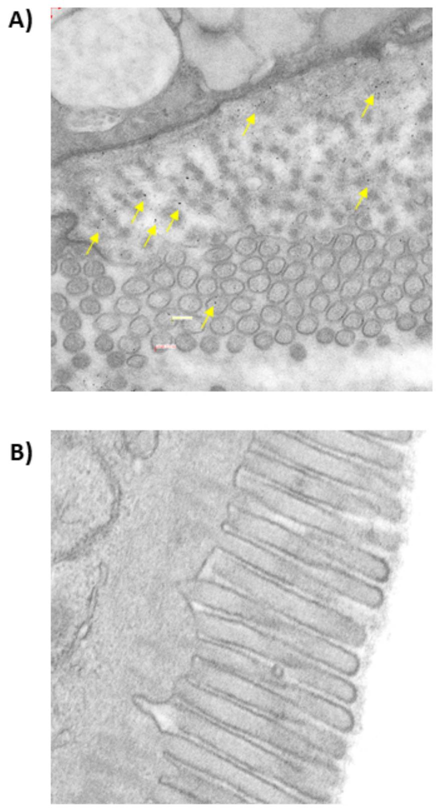

Figure 4

Figure 4

190x254mm (96 x 96 DPI)

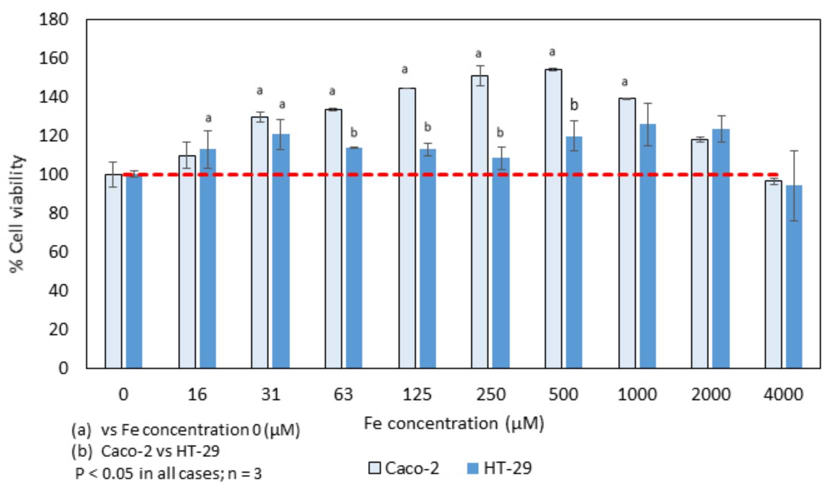

Figure 5

Figure 5

190x254mm (96 x 96 DPI)

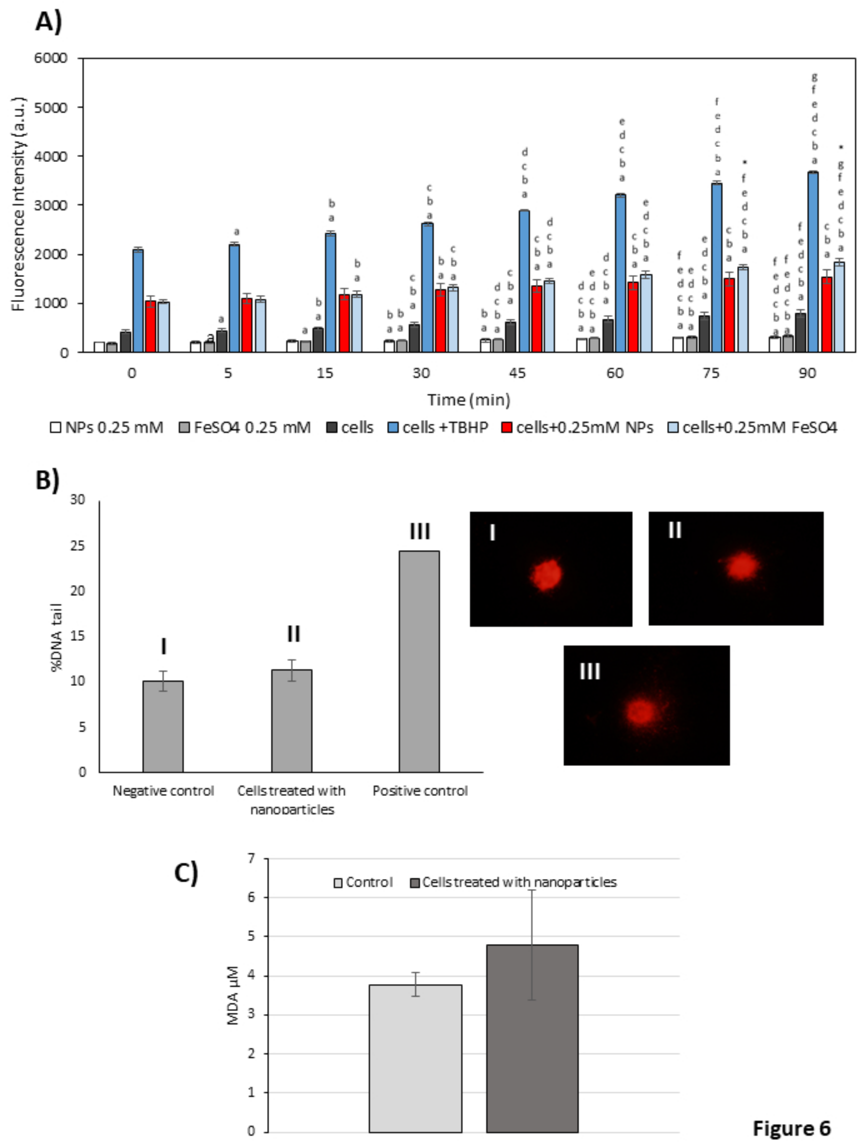

Figure 6

190x254mm (96 x 96 DPI)

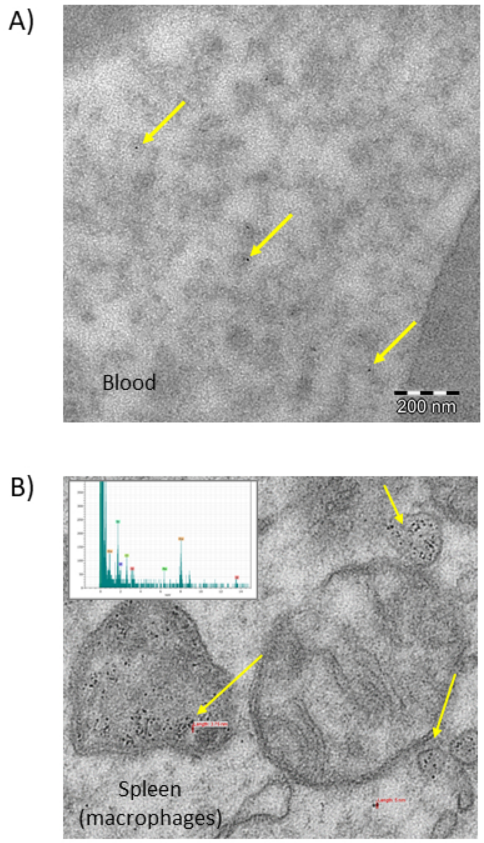

Figure 7

Figure 7

190x254mm (96 x 96 DPI)

SUPPLEMENTARY MATERIAL

In vivo and ex vivo experiments to evaluate the biodistribution and cellular toxicity of ultrasmall iron oxide nanoparticles potentially used as oral iron supplements.

J. García Fernández,[a,c] D. Turiel, J. Bettmer,[a] N. Jakubowski,[b] U. Panne,[b,c] , L. Rivas[d], J. Llopis[d], C. Sánchez González[d] and M. Montes-Bayón[a*]

[a] Department of Physical and Analytical Chemistry, Faculty of Chemistry, University of Oviedo, Julián Clavería 8, 33006 Oviedo, Spain

[b] BAM Federal Institute for Materials Research and Testing, Richard-Willstaetter Str. 11, 12489 Berlin, Germany

[c] Humboldt-University Berlin, School of Analytical Sciences Adlershof, Unter den Linden 6, 10099 Berlin, Germany

[d] Biomedical Research Centre, iMUDS, Institute of Nutrition and Food Technology "José Mataix", Department of Physiology, Faculty of Pharmacy, University of Granada, Campus Cartuja, 18071, Granada, Spain

*montesmaria@uniovi.es; Phone: +34-985103478

For Peer Review Only

Characterization of synthesized FeNPs

High Resolution-Transmission Electron Microscopy (HR-TEM) images were taken in a JEOL JEM-2100F (Tokyo, Japan) with TEM operation voltage at 200 kV to image iron NPs suspensions deposited on copper grids, and analyzed to obtain particle diameter average and check nanoparticle shape and aggregation. Figure S1 shows discrete particles with no visible aggregates. The average of core size is 3.65 ± 0.39 nm and homogeneous size distribution as well as spherical shape are observed.

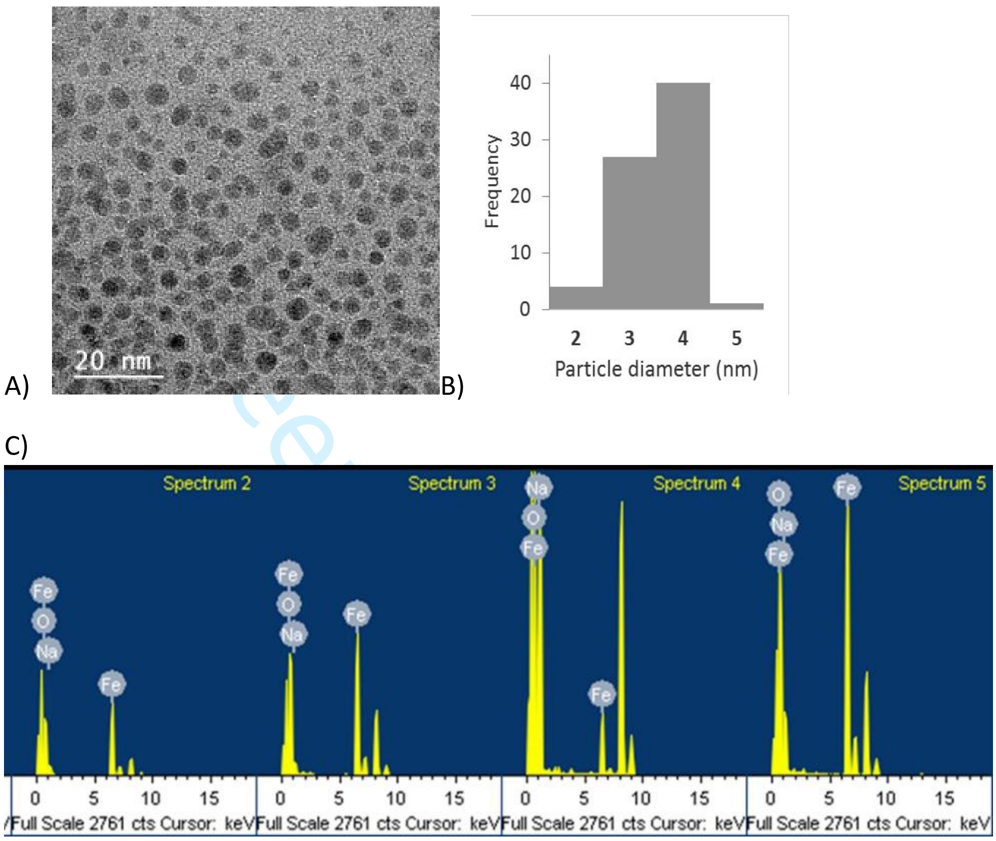

Figure S1: A) TEM image of the synthesized iron NPs, B) Histogram of the analyzed particles (85) and C) EDX spectrum of the particles.

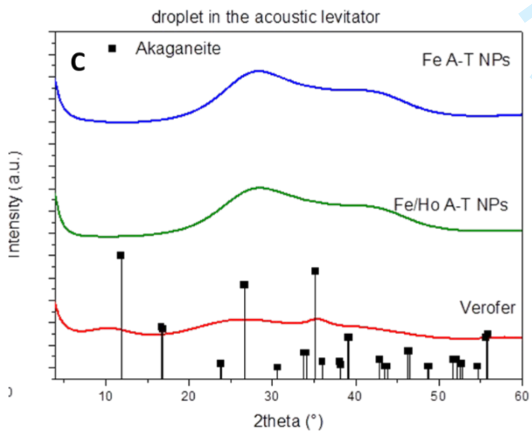

Figure S2: WAXS measurements of tartrate-modified NPs (blue line) and Holmium doped tartrate-modified NPs (green line) (in solution are represented with results for akaganeite structure that was expected with black squares).

Moreover, Dynamic Light Scattering (DLS) experiments were carried out in a Malvern Zetasizer Nano ZS (Malvern Instruments Ltd. Malvern, UK) with a detection angle of 173°. All measurements were taken at a temperature of 25ºC. Three replicates on each sample were taken to assess the repeatability of the measurements. The Nano S uses a 4 mW He–Ne laser operating at a wavelength of 633 nm. For the measurements, original samples were 100-fold diluted and ultrapure water was used. The dispersion in size as well as the NPs hydrodynamic diameter were assessed and the observed results are plotted in Figure S2A revealing that the hydrodynamic diameter is around 11.77 nm with a polydispersity index of 0.276. This means an acceptable monodispersing and homogeneity in this suspension and it can also be concluded that the modified tartrate coating corresponds to about 7-8 nm.

In addition, the results reveal that in the presence of "biological media" such as cell growing media, the particles tend to slightly aggregate to form, partially, entities with a size below 100 nm and in the range of 50-60 nm.

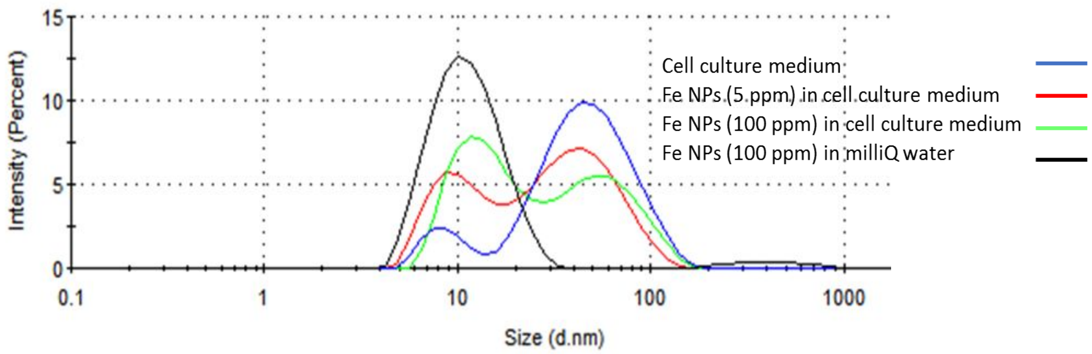

Figure S3: DLS results of different nanoparticle suspensions.

Optical absorption spectra were recorded using a Genesys 10S UV-vis spectrophotometer (Thermo Scientific, USA). A UV/Vis spectrum was obtained to evaluate the energy band gap of the semiconductor Fe-based nanomaterial.

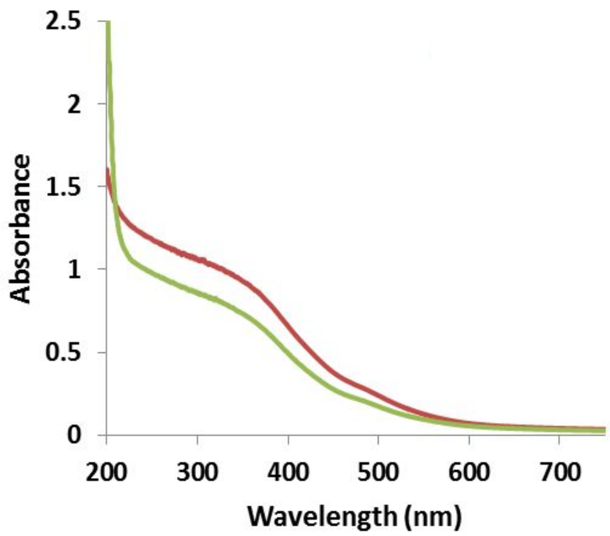

Figure S4: UV/Vis spectra of the synthesized iron nanoparticles.

The optical absorbance measurement was carried out at room conditions and Figure S4 shows the absorption profile obtained for synthesized FeNPs at two different dilutions. It appears as a continuous highly intensity band decreasing gradually at longer wavelengths. However, a high intensity band can be seen around 350 nm corroborating the presence of the oxo-metal charge transfer transition, expected in this kind of nanostructure in the range of 250-390 nm.

Histological integrity of the small intestine

The images show that the treatment with FeNP has not produced histological damage in the duodenum, jejunum or ileum, showing normal patterns in the mitochondria, intercellular junctions, microvilli and rest of cellular structures

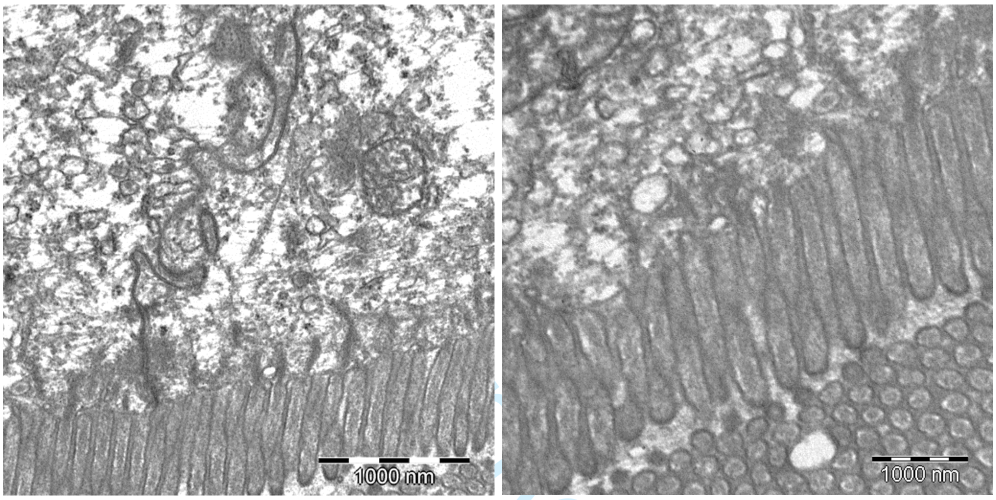

Figure S5: Normal histology of duodenum

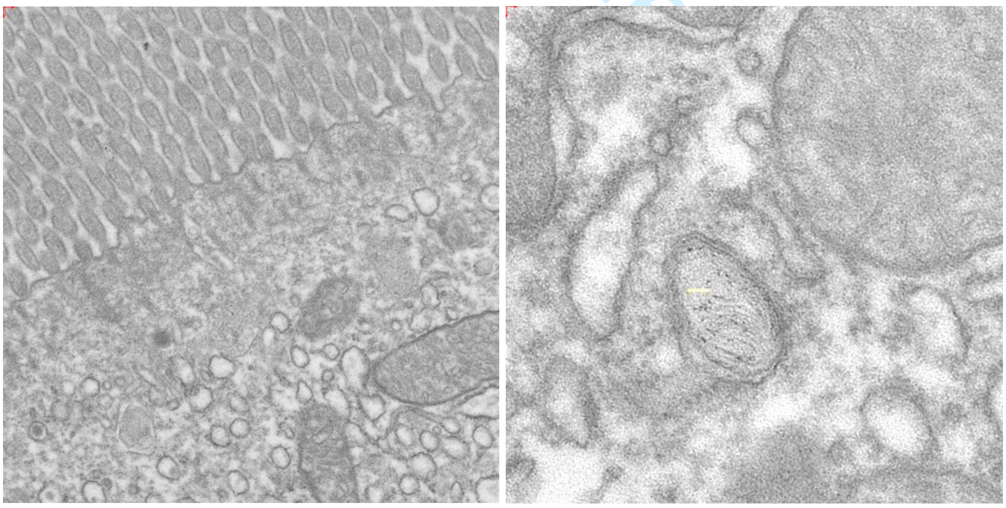

Figure S6: Normal histology of jejunum

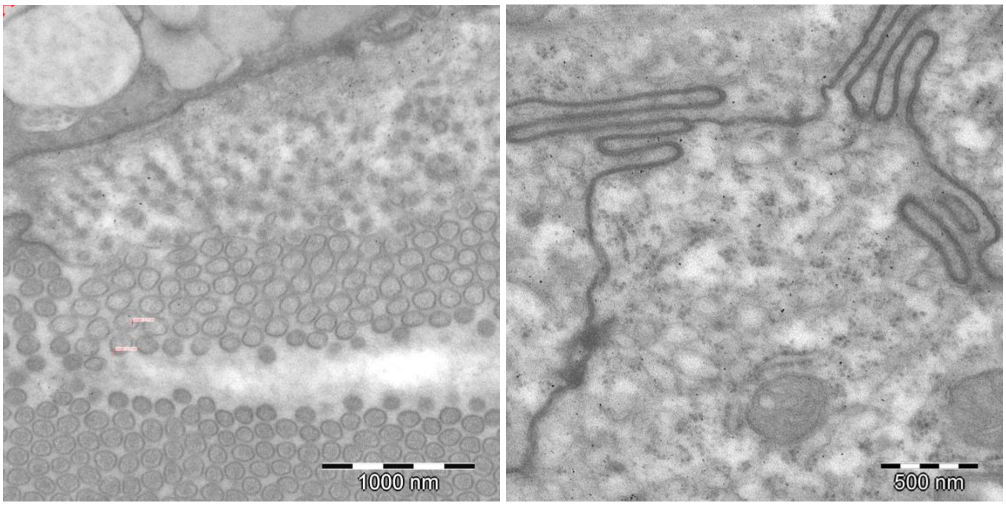

Figure S7: Normal histology of ileum

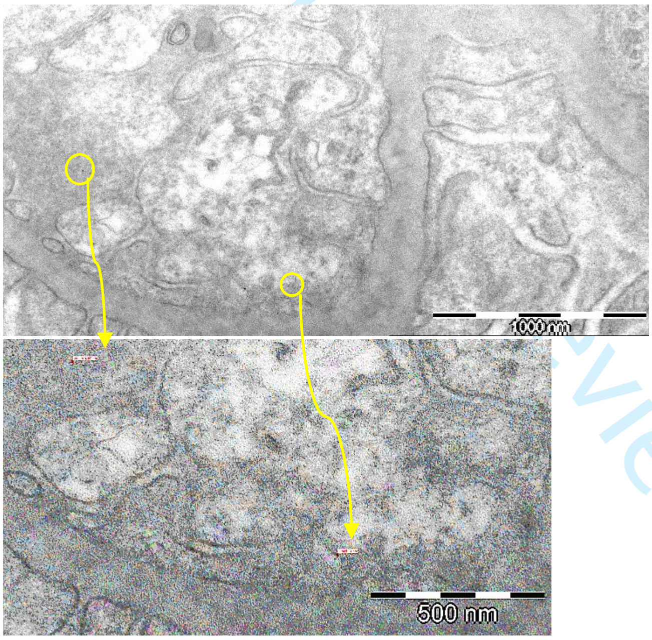

Figure S8: Histology of the kidney (glomerulus)

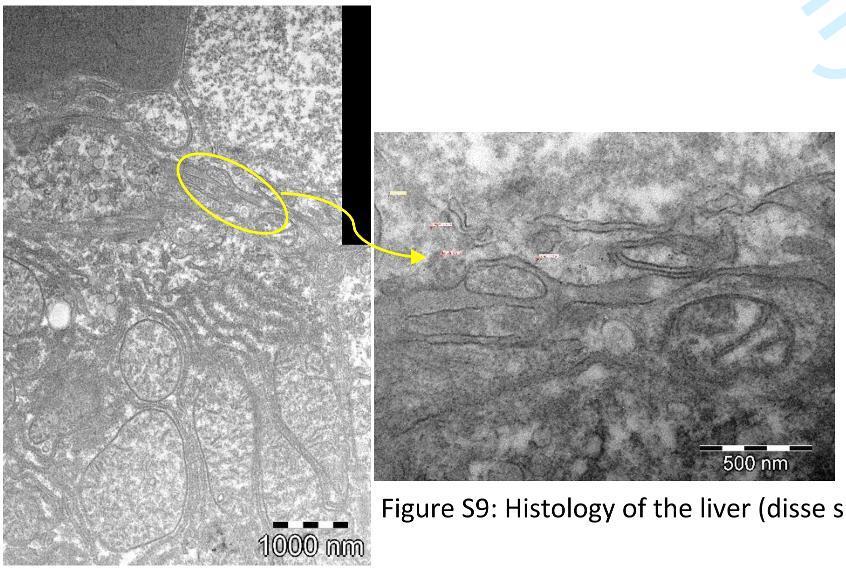

Figure S9: Histology of the liver (disse space)

For Peer Review Only

Table 1. ICP-MS operating conditions

Instrument	Agilent 7700	iCAP-TQ-ICP-MS
RF Power	1500 W	1550 W
Carrier gas flow rate	1.15 L·min^{-1}	0.8 L·min^{-1}
Coolant plasma gas flow rate	15 L·min^{-1}	14 L·min^{-1}
Reaction/collision gas flow	H_2	He
	3.5 mL·min^{-1}	7.8 mL·min^{-1}
Octapole bias	-18 V	-11.83 V
QP bias	-16 V	-
Nebulizer	Meinhard Type	Concentric
Spray chamber	Double pass, Peltier cooled (2^{o}C)	Cyclonic
m/z monitored	54, 56, 57	56, 57
Dwell time	0.1 s	0.1 s
Sensitivity (^{59}Co)	170.000 (cps/ppb)	300.000 (cps/ppb)

For Peer Review Only